PARM-1 staining showed cytoplasmic vesicular network pattern with intense perinuclear localization (Fig. 1D). When the cells were co-stained with anti-78 kDa glucose regulated protein/BiP (GRP78) antibody or MitoTracker, PARM-1 was co-localized with GRP78, an endoplasmic reticulum (ER)-resident chaperone, but not with MitoTracker, a mitochondrion-selective dye (Fig. 1D). Thus, PARM-1 is a transmembrane protein predominantly localized in ER in cardiac myocytes.

PARM-1 expression is increased in hearts of hypertensive heart disease

To investigate whether PARM-1 expression was regulated under pathological conditions in the postnatal hearts, we analyzed PARM-1 expression in the hearts of Dahl salt-sensitive rats. Dahl salt-sensitive rats were randomly assigned to receive either a 0.3% NaCl (low-salt) diet or an 8% NaCl (high-salt) diet at the age of 6 weeks. Consistent with the previous reports [10,11], upon a high-salt diet, Dahl salt-sensitive rats developed systemic hypertension, and a subsequent increase in left ventricular weight (LVW) to body weight (BW) ratio until 4 weeks after starting diet (Fig. 2A), indicating the development of left ventricular hypertrophy. Thereafter, a significant increase in lung weight (LW) to BW ratio and atrial weight (AW) to BW ratio was observed at 8 weeks (Fig. 2A), which was concomitant with a marked increase in atrial natriuretic factor (ANF) expression (Fig. 2B), suggesting the transition from hypertrophy to heart failure. In this model, PARM-1 expression was significantly increased at 8 weeks after starting diet, and reached more than 5 fold increase at 12 weeks (Fig. 2B). As ER stress is recently implicated in the pathogenesis of heart diseases such as ischemic heart disease and heart failure [12,13], we analyzed the expression of ER stress markers such as GRP78 and C/EBP homologous protein transcription factor (CHOP) in this model, and found that these ER stress markers were induced at the phase of transition from hypertrophy to heart failure (Fig. 2C).

Inflammatory cytokines and ER stress augment PARM-1 expression in cardiac myocytes

To explore how PARM-1 expression was regulated, cultured cardiac myocytes were stimulated by various hypertrophic stimuli or cytokines, and PARM-1 expression was analyzed by real time PCR. As shown in Fig. 3A, PARM-1 expression was stimulated by proinflammatory cytokines such as TGF-β, TNF-α and IL-1β, but not by hypertrophic stimuli such as phenylephrine, leukemia inhibitory factor and isoproterenol. Since ER stress developed in hypertensive heart failure (Fig. 2C), we also analyzed PARM-1 expression in ER stress conditions (Fig. 3B). Both thapsigargin and tunicamycin treatments led to induction of GRP78 and CHOP in cardiac myocytes. PARM-1 expression was markedly increased 24 hours after treatment with these ER stress inducers, and continued to be increased up to 48 hours (Fig. 3B). While thapsigargin and tunicamycin increased PARM-1 expression in a dose-dependent manner in cardiac myocytes, neither of them induced PARM-1 expression in cardiac fibroblasts (Fig. 3B), indicating PARM-1 induction by ER stress is also specific for cardiac myocytes. Treatment with thapsigargin and tunicamycin resulted in reduced viability in cardiac myocytes, and the effects were time- and dose-dependent (Fig. 3C).

Silencing PARM-1 augments apoptotic cell death induced by ER stress

To assess functional significance of PARM-1 induction in response to ER stress, PARM-1 expression was silenced by siRNA. We identified three different siRNAs, which efficiently silenced PARM-1 expression in cardiac myocytes (Fig. 4A). When PARM-1 expression was silenced by siRNA, ER stress-induced apoptotic response was significantly increased compared to control siRNA (Fig. 4B). Silencing PARM-1 expression further reduced cell viability in response to ER stress inducers. These results indicated that increased expression of PARM-1 in response to ER stress has a protective role in cardiac myocytes.

PARM-1 silencing decreases PERK and ATF6, and increases CHOP expression in ER stress condition

In the last set of experiments, we analyzed the effects of PARM-1 silencing on the signal transduction pathways mediating ER stress responses. In ER stress/unfolded protein response (UPR), misfolded proteins are first recognized by ER-resident chaperons such as GRP78. The status of protein folding in ER lumen is then sensed and transduced by three ER membrane proteins, PKR-like endoplasmic reticulum kinase (PERK), activating transcription factor 6 (ATF6) and endoribonuclease inositol-requiring enzyme-1 (IRE-1), each of which defines a distinct arm of ER stress responses [12,13,14]. Expression of GRP78, ATF6 and IRE-1, phosphorylation of PERK and mRNA splicing of XBP-1 were induced by ER stress inducers, thapsigargin or tunicamycin, in cardiac myocytes (Fig. 5A). Although silencing PARM-1 expression did not change GRP78 and IRE-1 expression, and XBP-1 splicing, expression of PERK and ATF6, and phosphorylation of PERK were markedly attenuated by PARM-1 silencing, only in the settings of ER stress (Fig. 5A). It has been shown that ER stress-induced apoptosis signal is mediated by increased expression of CHOP, and activation of Caspase-12 and c-Jun NH2-terminal kinase (JNK) [12,13,14]. While silencing of PARM-1 expression did not alter JNK and Caspase-12 activation, CHOP expression by ER stress inducers was significantly enhanced by PARM-1 silencing (Fig. 5B).

Discussion

In this study, we carried out the efficient signal sequence trap cloning using retrovirus-mediated gene transfer [6,9] to identify novel transmembrane and secreted molecules expressed in cardiac myocytes. Through this screening, several genes, which have not been widely recognized to be expressed in cardiac myocytes, were identified. These include PARM-1, glypican-1, podocalyxin-like and CD320 antigen, and our expression analysis verified that these genes were indeed expressed in cardiac myocytes (data not shown). As PARM-1 expression was most significantly modulated in the hearts of hypertensive heart disease model of Dahl salt-sensitive rats, we focused PARM-1 in this study. While changes in expression of other genes were not as marked as PARM-1 in this model (data not shown), changes in expression level could not designate the biological significance, and the roles of these other gene products in cardiac myocytes will be an important issue to be studied in the future studies.

PARM-1, also referred to as castration induced prostatic apoptosis-related protein 1 (Cipar1), is originally identified as a gene overexpressed in the prostate of castrated rats [8]. PARM-1 is expressed in the epithelial cells of involuting rat prostates after androgen removal, and the regulation of PARM-1 by androgen is limited to the prostates [8]. In contrast, in prostate cancer cell lines, and in human prostate cancer xenograft, CWR22, PARM-1 is constitutively expressed, and PARM-1 expression is positively regulated by androgen in CWR22 xenograft [15]. While the kinetics of PARM-1 expression is highly correlated with the development of apoptosis after castration, transient expression of

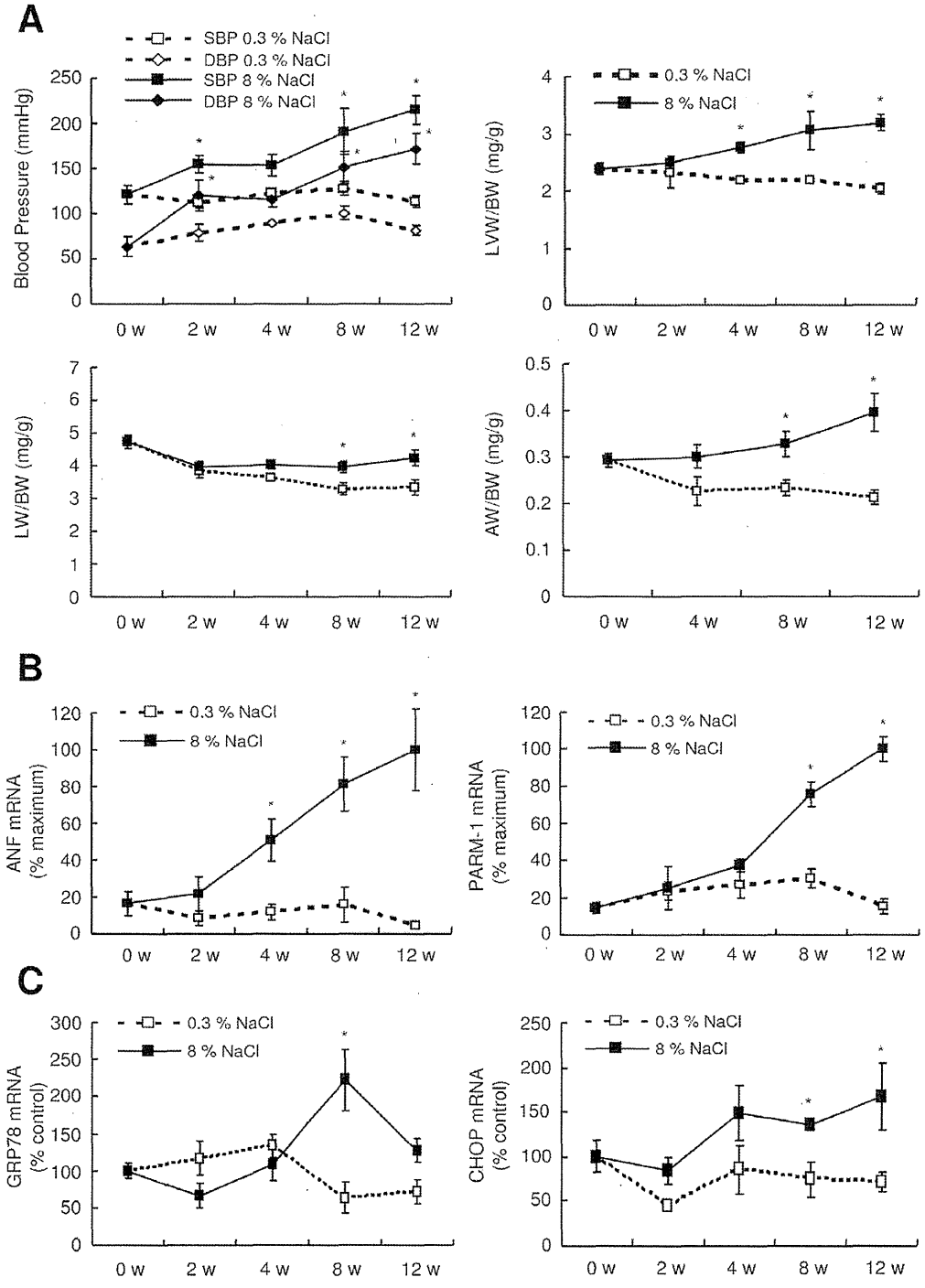

Figure 2. PARM-1 expression and ER stress response was activated in hypertensive heart disease model of Dahl salt-sensitive rats. *A*: The animals were subjected to a high- (8% NaCl, n = 12 for each time point) or low-salt diet (0.3% NaCl, n = 8 for each time point). Blood pressure and left ventricular weight (LVW), Body weight (BW), lung weight (LW) and atrial weight (AW) were measured at the indicated periods of time after starting the designated diet. *B, C*: ANF and PARM-1 expression (B), and ER stress markers such as GRP78 and CHOP (C) were analyzed by kinetic real-time PCR on cDNAs from the hearts of Dahl salt-sensitive rats. *$P<0.05$ versus a low-salt diet group at the respective time point.
doi:10.1371/journal.pone.0009746.g002

PARM-1 does not induce programmed cell death [8]. Although ectopic expression of human PARM-1 in a prostate cancer cell line results in increased colony formation [15], suggesting a probable role of PARM-1 in cell proliferation, the others reported that transient expression of rat PARM-1 does not alter the proliferative property of another prostate cancer cell line [16]. Thus, the

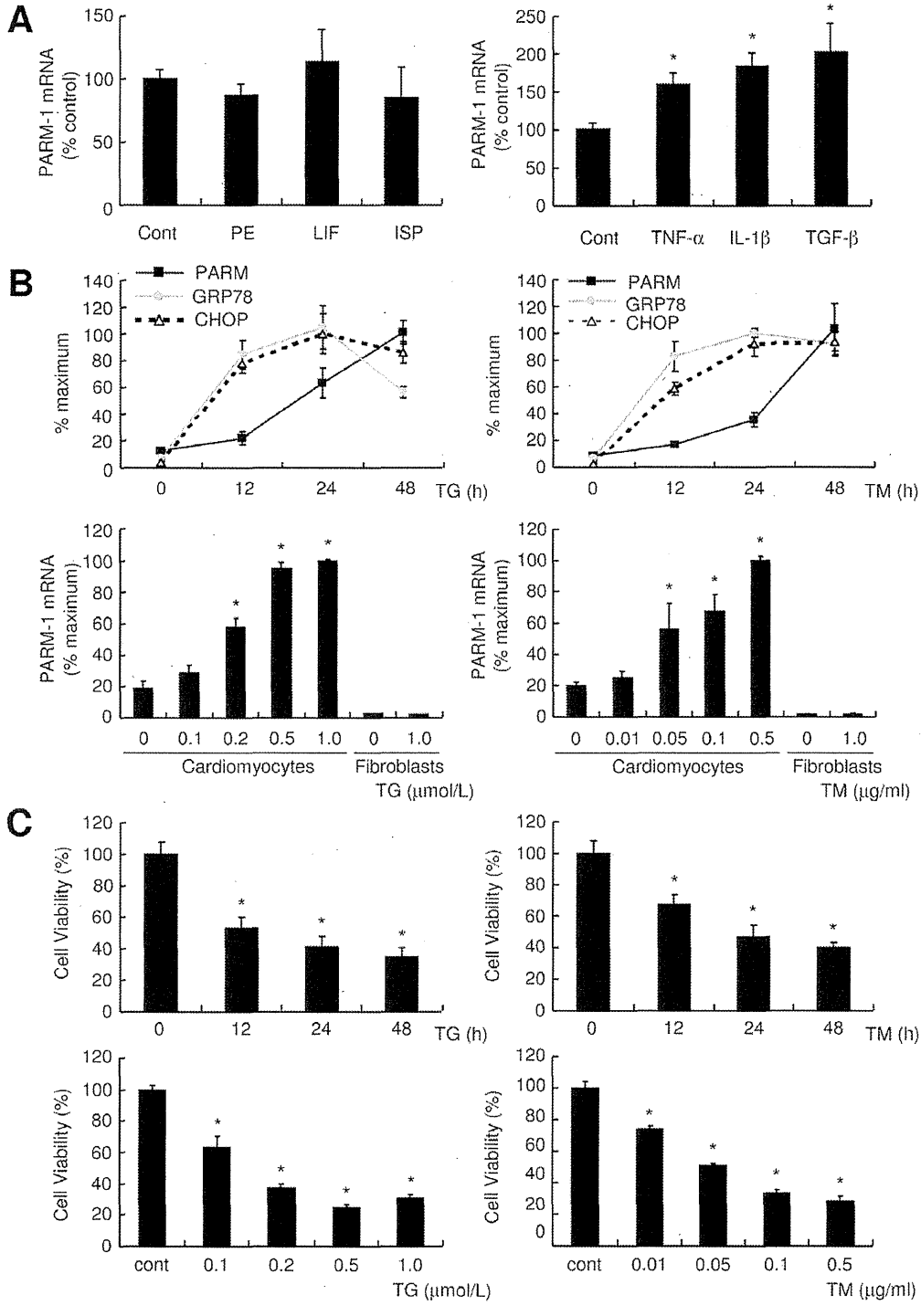

Figure 3. PARM-1 expression was induced by inflammatory cytokines and ER stress inducers specifically in cardiac myocytes. *A*: Cultured rat neonatal cardiac myocytes were stimulated by hypertrophic stimuli such as 100 μmol/l phenylephrine (PE), 1000 U/ml leukemia inhibitory factor (LIF) and 10 μmol/l isoproterenol (ISP), or inflammatory cytokines such as 100 ng/ml TNF-α, 5 ng/ml IL-1β and 4 ng/ml TGF-β. PARM-1 expression was analyzed 48 hours after stimulation. *B*: Cardiac myocytes were treated with 0.5 μmol/l thapsigargin (TG) or 0.1 μg/ml tunicamycin (TM) for the indicated periods of time, and GRP78, CHOP and PARM-1 expression was analyzed by kinetic real time PCR. *C*: Cardiac myocytes and fibroblasts were treated with TG or TM for 48 hours at the indicated concentration, and PARM-1 expression was analyzed. *D*: Cardiac myocytes were treated with TG or TM as indicated, and cell viability was assessed by WST-8 assay. *$P<0.05$ versus non-treated control cells.
doi:10.1371/journal.pone.0009746.g003

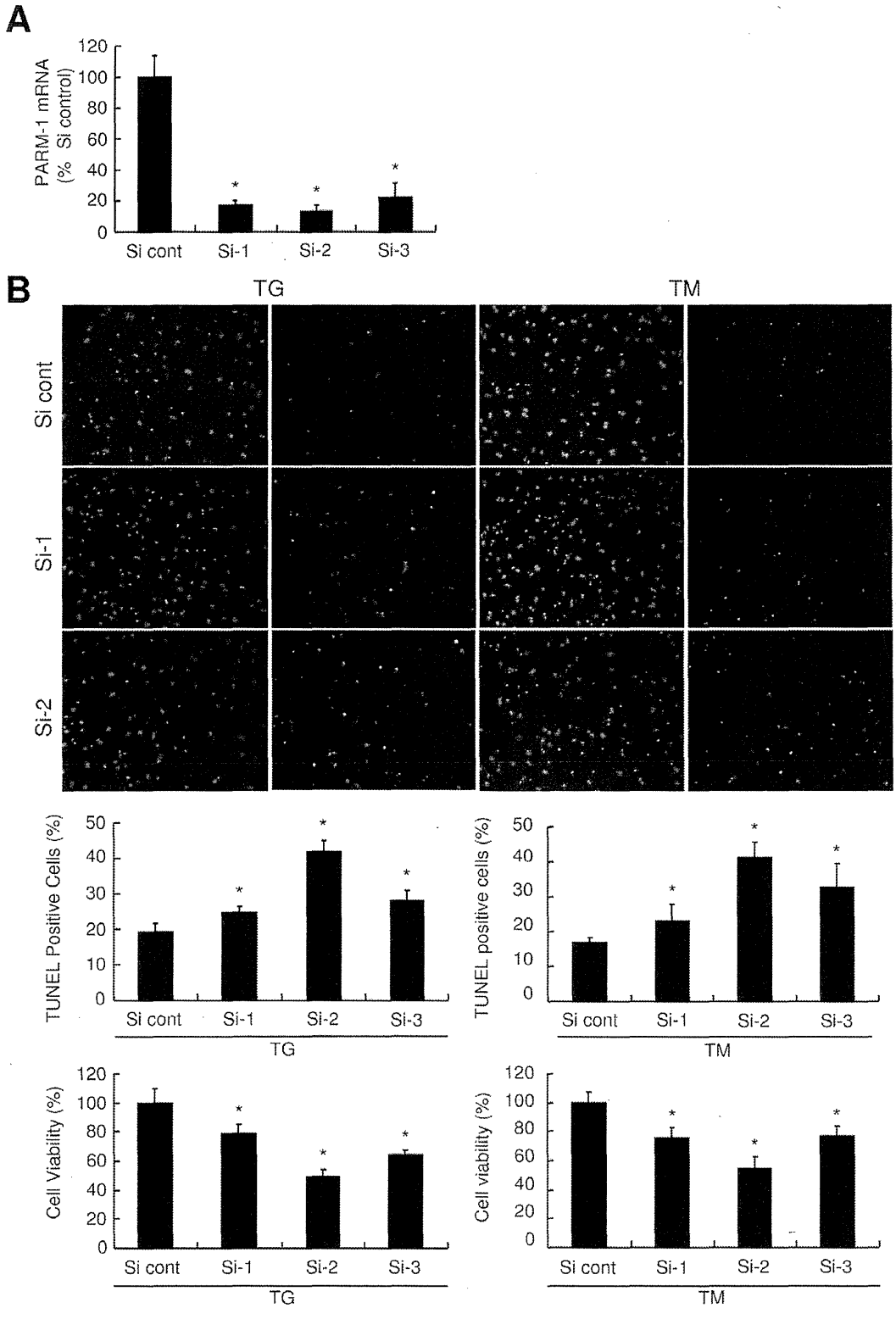

Figure 4. Silencing of PARM-1 augmented apoptotic response to ER stress. *A*: Cultured neonatal rat cardiac myocytes were transfected with 30 nmol/l of three different siRNA duplexes, and assessed for PARM-1 expression 24 hours after transfection. *B*: Cells were treated with TG or TM 72 hours after transfection with siRNAs for 24 hours. Apoptotic cell death was assessed by TUNEL assay, and cell viability was analyzed by WST-8 assay. *$P<0.05$ versus control siRNA (Si cont).
doi:10.1371/journal.pone.0009746.g004

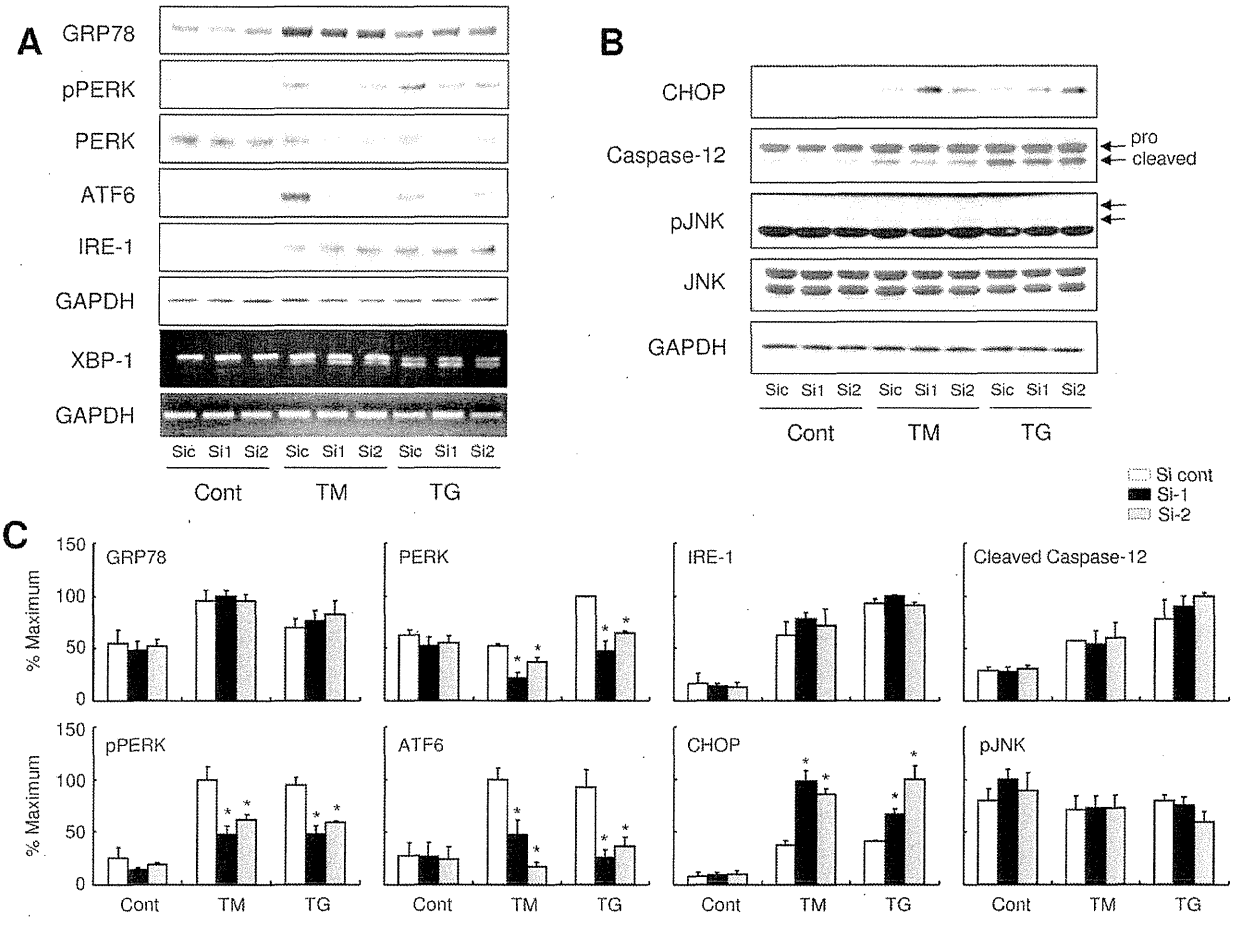

Figure 5. PARM-1 silencing decreases PERK and ATF6, and increases CHOP expression in ER stress condition. Cultured neonatal rat cardiac myocytes were transfected with siRNAs, and, after 72 hours, were treated with TM or TG for 48 hours. *A*: Immunoblot analysis was performed with antibody against GRP78, phospho-PERK, PERK, ATF6, IRE-1 or GAPDH. XBP-1 mRNA splicing was assessed by PCR. *B*: Immunoblot analysis was performed with antibody against CHOP, Caspase-12, phospho-JNK, JNK or GAPDH. *C*: Densitometric analysis was carried out using ImageJ software. The results were normalized against GAPDH, and expressed as percentages of the maximum. *$P<0.05$ versus control siRNA (Si cont) of respective treatment with TM or TG.
doi:10.1371/journal.pone.0009746.g005

regulation of PARM-1 especially in other organs than prostate, and its roles are largely unknown.

Our analysis on hypertensive heart disease model of Dahl salt-sensitive rats demonstrated that PARM-1 expression was significantly upregulated following a high-salt diet. While one of the early cardiac manifestations of this model is hypertension-induced cardiac hypertrophy [10,11], PARM-1 expression was unchanged 4 weeks after starting a high-salt diet, when a significant increase in LVW to BW ratio was already detected (Fig. 2A,B). Further, in cultured cardiac myocytes, stimulation with hypertrophic stimuli did not alter the expression of PARM-1 (Fig. 3A). This could be in accordance with PARM-1 expression in the hearts during normal developmental stages. While a common feature of various hypertrophic responses is re-activation of fetal gene programs such as ANF and skeletal α-actin genes [17], PARM-1 expression readily detectable at E10.5 was increased toward neonatal stages, and then maintained through adult stages (Fig. 1C). These results suggested that PARM-1 expression could not be a part of fetal gene programs or hypertrophic responses. Another feature of hypertensive heart disease is a development of heart failure. In our model, 8 weeks after staring a high-salt diet, a significant increase in LW to BW ratio was observed, indicating the presence of lung congestion. Although we did not detected a significant increase in LV dimension and a decrease in fractional shortening up to 12 weeks of a high-salt diet (data not shown), a significant increase in AW to BW ratio was noted at 8 weeks, suggesting the development of diastolic heart failure in this model. In this model, PARM-1 was significantly upregulated 8 weeks after starting a high-salt diet, suggesting that PARM-1 was induced in the setting of heart failure. Development of heart failure involves neurohumoral and inflammatory mechanisms [18,19], and recent evidences have suggested that ER stress plays an important role in the pathogenesis of heart failure [12,13]. In cultured cardiac myocytes, inflammatory cytokines stimulated PARM-1 expression (Fig. 3A). Further, ER stress inducers, thapsigargin and tunicamycin markedly upregulated PARM-1 expression (Fig. 3B), and ER stress markers such as GRP78 and CHOP were also upregulated in the hearts of hypertensive heart disease model at the heart failure phase (Fig. 2C). These results implied that PARM-1 expression is upregulated during heart failure, involving inflammatory cytokines and ER stress.

As PARM-1 was localized in ER in cardiac myocytes, and ER stress induced PARM-1 expression, PARM-1 could play a role in ER stress response. ER is a cellular organelle, where protein synthesis and folding of secreted and transmembrane proteins take place. When ER environment is perturbed, and the folding of nascent proteins is impaired, a quality control system called UPR is activated [12,13,14]. Initially, UPR is an adaptive response in which the cells attempt to overcome the accumulation of misfolded proteins through augmenting protein folding capacity. However, when ER stress is excessive and prolonged, cells undergo apoptotic cell death. Thus, ER stress response has a conditional ability to protect the cells or activate cell death program. In the hearts, ER stress response has been shown to be activated in several pathological models including myocardial infarction, ischemia/reperfusion and pressure overload-induced hypertrophy [20,21,13,22]. Pressure overload by transverse aortic constriction has been shown to induce prolonged ER stress during the transition from cardiac hypertrophy to heart failure [20]. AMP-activated protein kinase protects cardiac myocytes from hypoxic injury by attenuating ER stress [23]. Aberrant ER quality control in transgenic mice with mutant KDEL receptor, or chronic myocardial inflammation induced by chemoattractant protein-1 transgene activates ER stress response and causes heart failure [24,25]. These results indicated that ER stress response could be deleterious in the hearts. In contrast, overexpression of ER stress gene GRP94 protects cardiac myocytes from oxidative injury [26], and inducible transgene of activated form of ATF6 in the hearts protects the hearts from ischemia/reperfusion damage [27], suggesting the protective role of ER stress response in the hearts. Thus, the outcome of ER stress response is also context dependent in the heart. In our model of hypertensive heart disease, ER stress response assessed by the expression of GRP78 and CHOP was activated in the phase of transition from hypertrophy to heart failure (Fig. 2C). While GRP78 expression reached a peak at 8 weeks of diet and then declined, CHOP expression remained upregulated until 12 weeks. Those expression patterns might be compatible with those reported in transverse aortic constriction-induced heart failure model, as a peak expression of GRP78 is observed at 1 week after transverse aortic constriction, while CHOP is upregulated even at 4 weeks [20]. Since induction of ER chaperone GRP78 represents a major survival arm of ER stress response, and indeed, overexpression of ER chaperone is protective for cardiac myocytes from ischemia and calcium overload injuries [26], these observations could be in good accordance with the general view that the UPR has a protective role during initial phase of ER stress, while proapoptotic pathways are activated upon continued ER stress [12,13,14]. Thus, ER stress response in our model might have the deleterious effect in the transition to heart failure, while it is still possible that this ER stress response was a part of counteracting efforts against developing heart failure.

Consistent with the contradictory roles of ER stress response in cell survival and death, ER stress has been demonstrated to activate both prosurvival and apoptotic signaling pathways [13,14]. In cultured cardiac myocytes, treatment of cardiac myocytes with ER stress inducers resulted in reduced viability and increased apoptotic cell death [20]. In this setting, PARM-1 expression was markedly increased (Fig. 3B), and silencing PARM-1 expression significantly augmented ER stress-induced cell death (Fig. 4B), indicating PARM-1 is a part of cell survival pathways in ER stress response. Given that PARM-1 expression was induced in the phase of transition to heart failure in hypertensive heart disease model of Dahl salt-sensitive rats (Fig. 2B), the increased expression of PARM-1 in this model could play a role to counteract against development of heart failure through inhibiting apoptosis of cardiac myocytes, although further studies are needed to determine the role of PARM-1 induction in the development of heart failure in vivo.

ER stress is sensed by three distinct ER sensory proteins, PERK, ATF6 and IRE-1, which are kept inactivated by binding with ER-resident chaperones such as GRP78 and GRP94. Upon accumulation of misfolded proteins in ER, the chaperones are occupied by misfolded proteins, which results in the release and activation of the ER stress sensors, and subsequent activation of downstream signaling pathways [12,13,14]. The downstream signaling effectors include prosurvival and proapoptotic pathways, and it is anticipated that the balance between prosurvival and proapoptotic pathways determines the ultimate outcome of ER stress response, while the precise molecular mechanisms involved in cell fate determination remain to be delineated. In this study, silencing of PARM-1 did not alter the expression of GRP78, suggesting the expression of PARM-1 was not involved in the regulation of ER stress itself, or expression of ER chaperones (Fig. 5A). Downregulation of PARM-1 expression by siRNA markedly attenuated the expression of PERK and ATF6 without affecting IRE1 induction and XBP-1 splicing. Interestingly, these effects of PARM-1 silencing on PERK and ATF6 expression were only observed upon stimulation with thapsigargin or tunicamycin (Fig. 5). These results suggested that PARM-1 plays a crucial role in maintaining PERK and ATF6 expression in the setting of ER stress conditions. Since overall PERK signaling is protective against cell death in most circumstances [13,14,28], and preactivation of ATF6 protects the heart against ischemia/reperfusion insult [27], maintenance of PERK and ATF6 expression by PARM-1 is critical for cardiac myocytes to cope with ER stresses. The CHOP, JNK and Caspases are distal effectors of ER stress response that have been implicated in mediating apoptotic signals. CHOP induction was markedly augmented by PARM-1 silencing, while activation of JNK and Caspase-12 was unaffected (Fig. 5B,C), indicating that PARM-1 was also mediating prosurvival effect by suppressing CHOP-mediated apoptotic pathways in cardiac myocytes. Expression of CHOP, but not activation of JNK and Caspase-12 has been shown to be induced by transverse aortic constriction in murine hearts [20]. In cultured cardiac myocytes, proteasome inhibitors are shown to activate ER stress response and apoptosis, in which silencing CHOP, but not inhibition of JNK or Caspase-12 rescues cardiac myocytes from apoptosis [29]. Thus, CHOP expression might be one of important mechanisms inducing cardiac myocyte apoptosis in response to ER stress, and PARM-1 has an inhibitory role in this pathway. As CHOP is known to be regulated downstream of PERK and ATF-6 [30,13,28], and PARM-1 is involved in the maintenance of PERK and ATF-6 without affecting IRE-1 induction and XBP-1 splicing, it looks likely that PARM-1 is involved in a specific set of signal transduction pathways in ER stress response, while further studies are clearly needed to delineate the molecular mechanisms by which PARM-1 regulates ER stress response pathways.

An intriguing finding of this study was PARM-1 expression and induction of PARM-1 by ER stress was specific for cardiac myocytes (Fig. 3B). Recently, several ER membrane molecules specific for certain cell types have been identified. Those include CREB4, CREB-H, Luman and OASIS, and are involved in ER stress response [31,32,33,34]. For example, CREB-H is expressed exclusively in the liver [35], and activated by ER stress [34]. However, ER stress-induced activation of CREB-H leads to induction of acute phase response genes such as C-reactive protein and serum amyloid P-component rather than canonical unfolded

protein responses [34]. Thus, ER stress response could have specialized roles in specialized cells. Although there is a striking difference between those molecules and PARM-1, as those belong to basic-leucine zipper transcription factor, and PARM-1 does not have any known domain for transcription factors, PARM-1 could mediate ER stress response specific for cardiac myocytes.

In this study, we identified PARM-1 as an ER protein specifically expressed in cardiac myocytes, and found that PARM-1 expression was induced in hypertensive heart disease model, and by ER stress in cardiac myocytes. Further, it was also shown that PARM-1 had a protective role against ER stress-induced apoptotic response in cardiac myocytes. As elucidation of cardiac specific ER stress response could have therapeutic impacts on many heart diseases, identification of molecular mechanisms regulated by PARM-1 will be an important issue to understand cardiac specific ER stress responses.

Materials and Methods

Cardiac myocytes culture

Neonatal rat cardiac myocytes and non-myocytes were prepared from 1-day-old Wistar rat hearts as described previously [36,37]. Neonatal rat ventricles were enzymatically digested, and cardiac myocytes were purified over a discontinuous Percoll gradient. Cardiac myocytes were cultured in DMEM/F-12 medium supplemented with 5% fetal bovine serum and 100 μmol/l 5-bromo-2-deoxyuridine (BrdU) for 16-24 hours, and culture medium was then changed to serum-deprived medium containing insulin, transferrin, selenium, bovine serum albumin and BrdU. Non-myocytes in the upper layer were plated onto non-coated culture dishes, and the attached cells were cultured and passaged. Non-myocytes at 2nd passage were used for the experiments. Each experiment was performed under serum free condition at least 24 hrs after serum deprivation.

Signal sequence trap

Signal sequence trap by retrovirus-mediated expression screening (SST-REX) was performed as previously described [6,9]. Briefly, a library was constructed in the retrovirus vector pMX-SST employing cDNA derived from poly(A)$^+$ RNA isolated from neonatal rat cardiac myocytes. The interleukin-3 (IL-3)-dependent pro-B cell line Ba/F3 [6,9] was infected with retrovirus, followed by seeding onto 96-multiwell plates in the absence of IL-3. Genomic DNA extracted from IL-3-independent Ba/F3 clones were subjected to PCR to recover the integrated cDNAs using primers specific for the cloning vector. After electrophoresis of the PCR products, DNA was recovered and subjected to sequencing.

Animals and treatments

Male Dahl salt-sensitive rats (6 weeks old) were purchased from Shimizu laboratory supplies. From 6 weeks onwards, these rats were fed a high-sodium diet (containing 8% NaCl) or a low-sodium diet (containing 0.3% NaCl) [10,11]. After 2, 4, 8 and 12 weeks, blood pressure was measured by the tail-cuff method. All procedures using animals performed in this study were approved by the Institutional Animal Care and Use Committee of Kyoto Prefectural University of Medicine.

Reverse transcriptase (RT)-PCR

Total RNA was extracted from rat tissues using TRIzol (Invitrogen) and from neonatal rat cardiac myocytes using the RNeasy mini kit (Qiagen), and then cDNA was synthesized by the High Capacity cDNA Reverse Transcription Kit (Applied Biosystems). Synthesized cDNA was analyzed by quantitative kinetic real-time PCR using the ABI Prism 7700 Sequence Detector system (Applied Biosystems) with SYBR Premix Ex Taq (Takara) [38,39]. Rat glyceraldehyde-3-phosphate dehydrogenase (GAPDH) was used for normalization, and the comparative threshold (C_T) method was used to assess the relative abundance of the targets. For XBP-1 mRNA splicing, the primers flanking the intron splicing site by IRE-1 was used for PCR, and the products were analyzed by agarose gel electrophoresis with visualization using ethidium bromide [40].

Immunostaining

Cells were stained with anti-flag M2 monoclonal antibody (Sigma) or goat polyclonal antibody against GRP78 (Santa Cruz), followed by Alexa Fluor 488- or Alexa Fluor 555-conjugated secondary antibody (Invitrogen). Mitochondria were stained with MitoTracker Green FM (Invitrogen) and nuclei were visualized using DAPI. Images were captured with a BZ-8000 microscope (Keyence).

Immunoblot analysis

Cells lysates normalized by protein concentration were subjected to 10% or 15% SDS-polyacrylamide gel electrophoresis, and transferred to polyvinylidene difluoride membranes (Millipore) [38,39]. Blots were immunoblotted with the primary antibody against GRP78, CHOP (Santa Cruz), phospho-PERK, PERK, IRE-1, phospho-JNK, JNK (Cell Signaling), Caspase-12 (Sigma) or ATF6 (AnaSpec), and horseradish peroxidase-labeled donkey secondary antibody, followed by enhanced chemiluminescence (GE Healthcare). Densitomeric analysis was performed using ImageJ software.

Small interfering RNA–mediated silencing

PARM-1 stealth siRNA duplexes were purchased from Invitrogen. Target sequences of siRNA are: siRNA-1; 5′-GAACACAGTCTCGGCAGTCCTGAAA-3′, siRNA-2; 5′-TCCGCTTCCGTTACCTCTAACCACA-3′, siRNA-3; 5′-GCGGCATATCTGAAGATCAGGCATT-3′. Cells were transfected with 30 nmol/L siRNA duplex using Lipofectamine RNAiMAX reagent (Invitrogen) according to the manufacture's instruction [41]. Stealth RNAi negative control (Invitrogen) was used as a control.

Cell viability and TUNEL assay

Cell viability was assessed using WST-8 (2-(2-methoxy-4-nitrophenyl)-3-(4-nitrophenyl)-5-(2,4-disulfophenyl)-2H-tetrazolium, monosodium salt) (Kishida Kagaku) according to the manufacturer's instruction. Apoptotic cells were detected by *in situ* terminal deoxynucleotidyl transferase-mediated biotinylated UTP nick end labeling (TUNEL) assay using ApopTag Red In Situ Apoptosis Detection Kit (Chemicon) as previously described [39]. Cells were nuclear stained with DAPI, and the TUNEL positive and total nuclei were counted under the fluorescent microscope (IX71, Olympus Corporation) in 5 view fields per well.

Statistical analysis

All experiments were performed at least three times in duplicates. Data were expressed as means ± standard errors and analyzed by unpaired Student's *t*-test for comparisons between two groups, or one-way ANOVA with post hoc analysis for multiple comparisons. A value of $p<0.05$ was considered statistically significant.

Acknowledgments

We thank M. Nakata and M. Kuramoto for expert technical assistance.

Author Contributions

Conceived and designed the experiments: KI TT TU HO HM. Performed the experiments: KI TT HI NN TO SA AA. Analyzed the data: KI TT HI NN. Wrote the paper: KI TT.

References

1. Jessup M, Brozena S (2003) Heart failure. N Engl J Med 348: 2007–2018.
2. Neubauer S (2007) The failing heart–an engine out of fuel. N Engl J Med 356: 1140–1151.
3. Fisher SA, Langille BL, Srivastava D (2000) Apoptosis during cardiovascular development. Circ Res 87: 856–864.
4. Dorn GW, 2nd (2009) Apoptotic and non-apoptotic programmed cardiomyocyte death in ventricular remodelling. Cardiovasc Res 81: 465–473.
5. Lee Y, Gustafsson AB (2009) Role of apoptosis in cardiovascular disease. Apoptosis 14: 536–548.
6. Kojima T, Kitamura T (1999) A signal sequence trap based on a constitutively active cytokine receptor. Nat Biotechnol 17: 487–490.
7. Tashiro K, Nakamura T, Honjo T (1999) The signal sequence trap method. Methods Enzymol 303: 479–495.
8. Bruyninx M, Hennuy B, Cornet A, Houssa P, Daukandt M, et al. (1999) A novel gene overexpressed in the prostate of castrated rats: hormonal regulation, relationship to apoptosis and to acquired prostatic cell androgen independence. Endocrinology 140: 4789–4799.
9. Ogata T, Ueyama T, Nomura T, Asada S, Tagawa M, et al. (2007) Osteopontin is a myosphere-derived secretory molecule that promotes angiogenic progenitor cell proliferation through the phosphoinositide 3-kinase/Akt pathway. Biochem Biophys Res Commun 359: 341–347.
10. Doi R, Masuyama T, Yamamoto K, Doi Y, Mano T, et al. (2000) Development of different phenotypes of hypertensive heart failure: systolic versus diastolic failure in Dahl salt-sensitive rats. J Hypertens 18: 111–120.
11. Klotz S, Hay I, Zhang G, Maurer M, Wang J, et al. (2006) Development of heart failure in chronic hypertensive Dahl rats: focus on heart failure with preserved ejection fraction. Hypertension 47: 901–911.
12. Wang X, Robbins J (2006) Heart failure and protein quality control. Circ Res 99: 1315–1328.
13. Glembotski CC (2007) Endoplasmic reticulum stress in the heart. Circ Res 101: 975–984.
14. Lai E, Teodoro T, Volchuk A (2007) Endoplasmic reticulum stress: signaling the unfolded protein response. Physiology (Bethesda) 22: 193–201.
15. Fladeby C, Gupta SN, Barois N, Lorenzo PI, Simpson JC, et al. (2008) Human PARM-1 is a novel mucin-like, androgen-regulated gene exhibiting proliferative effects in prostate cancer cells. Int J Cancer 122: 1229–1235.
16. Cornet AM, Hanon E, Reiter ER, Bruyninx M, Nguyen VH, et al. (2003) Prostatic androgen repressed message-1 (PARM-1) may play a role in prostatic cell immortalisation. Prostate 56: 220–230.
17. Barry SP, Davidson SM, Townsend PA (2008) Molecular regulation of cardiac hypertrophy. Int J Biochem Cell Biol 40: 2023–2039.
18. Blum A, Miller H (2001) Pathophysiological role of cytokines in congestive heart failure. Annu Rev Med 52: 15–27.
19. Conraads VM, Bosmans JM, Vrints CJ (2002) Chronic heart failure: an example of a systemic chronic inflammatory disease resulting in cachexia. Int J Cardiol 85: 33–49.
20. Okada K, Minamino T, Tsukamoto Y, Liao Y, Tsukamoto O, et al. (2004) Prolonged endoplasmic reticulum stress in hypertrophic and failing heart after aortic constriction: possible contribution of endoplasmic reticulum stress to cardiac myocyte apoptosis. Circulation 110: 705–712.
21. Thuerauf DJ, Marcinko M, Gude N, Rubio M, Sussman MA, et al. (2006) Activation of the unfolded protein response in infarcted mouse heart and hypoxic cultured cardiac myocytes. Circ Res 99: 275–282.
22. Qi X, Vallentin A, Churchill E, Mochly-Rosen D (2007) δPKC participates in the endoplasmic reticulum stress-induced response in cultured cardiac myocytes and ischemic heart. J Mol Cell Cardiol 43: 420–428.
23. Terai K, Hiramoto Y, Masaki M, Sugiyama S, Kuroda T, et al. (2005) AMP-activated protein kinase protects cardiomyocytes against hypoxic injury through attenuation of endoplasmic reticulum stress. Mol Cell Biol 25: 9554–9575.
24. Azfer A, Niu J, Rogers LM, Adamski FM, Kolattukudy PE (2006) Activation of endoplasmic reticulum stress response during the development of ischemic heart disease. Am J Physiol Heart Circ Physiol 291: H1411–1420.
25. Szegezdi E, Duffy A, O'Mahoney ME, Logue SE, Mylotte LA, et al. (2006) ER stress contributes to ischemia-induced cardiomyocyte apoptosis. Biochem Biophys Res Commun 349: 1406–1411.
26. Vitadello M, Penzo D, Petronilli V, Michieli G, Gomirato S, et al. (2003) Overexpression of the stress protein Grp94 reduces cardiomyocyte necrosis due to calcium overload and simulated ischemia. FASEB J 17: 923–925.
27. Martindale JJ, Fernandez R, Thuerauf D, Whittaker R, Gude N, et al. (2006) Endoplasmic reticulum stress gene induction and protection from ischemia/reperfusion injury in the hearts of transgenic mice with a tamoxifen-regulated form of ATF6. Circ Res 98: 1186–1193.
28. Ron D, Walter P (2007) Signal integration in the endoplasmic reticulum unfolded protein response. Nat Rev Mol Cell Biol 8: 519–529.
29. Fu HY, Minamino T, Tsukamoto O, Sawada T, Asai M, et al. (2008) Overexpression of endoplasmic reticulum-resident chaperone attenuates cardiomyocyte death induced by proteasome inhibition. Cardiovasc Res 79: 600–610.
30. Yoshida H, Okada T, Haze K, Yanagi H, Yura T, et al. (2000) ATF6 activated by proteolysis binds in the presence of NF-Y (CBF) directly to the cis-acting element responsible for the mammalian unfolded protein response. Mol Cell Biol 20: 6755–6767.
31. Raggo C, Rapin N, Stirling J, Gobeil P, Smith-Windsor E, et al. (2002) Luman, the cellular counterpart of herpes simplex virus VP16, is processed by regulated intramembrane proteolysis. Mol Cell Biol 22: 5639–5649.
32. Kondo S, Murakami T, Tatsumi K, Ogata M, Kanemoto S, et al. (2005) OASIS, a CREB/ATF-family member, modulates UPR signalling in astrocytes. Nat Cell Biol 7: 186–194.
33. Stirling J, O'Hare P (2006) CREB4, a transmembrane bZip transcription factor and potential new substrate for regulation and cleavage by S1P. Mol Biol Cell 17: 413–426.
34. Zhang K, Shen X, Wu J, Sakaki K, Saunders T, et al. (2006) Endoplasmic reticulum stress activates cleavage of CREBH to induce a systemic inflammatory response. Cell 124: 587–599.
35. Omori Y, Imai J, Watanabe M, Komatsu T, Suzuki Y, et al. (2001) CREB-H: a novel mammalian transcription factor belonging to the CREB/ATF family and functioning via the box-B element with a liver-specific expression. Nucleic Acids Res 29: 2154–2162.
36. Horio T, Nishikimi T, Yoshihara F, Nagaya N, Matsuo H, et al. (1998) Production and secretion of adrenomedullin in cultured rat cardiac myocytes and nonmyocytes: stimulation by interleukin-1β and tumor necrosis factor-α. Endocrinology 139: 4576–4580.
37. Ogata T, Ueyama T, Isodono K, Tagawa M, Takehara N, et al. (2008) MURC, a muscle-restricted coiled-coil protein that modulates the Rho/ROCK pathway, induces cardiac dysfunction and conduction disturbance. Mol Cell Biol 28: 3424–3436.
38. Kitamura R, Takahashi T, Nakajima N, Isodono K, Asada S, et al. (2007) Stage-specific role of endogenous Smad2 activation in cardiomyogenesis of embryonic stem cells. Circ Res 101: 78–87.
39. Asada S, Takahashi T, Isodono K, Adachi A, Imoto H, et al. (2008) Downregulation of Dicer expression by serum withdrawal sensitizes human endothelial cells to apoptosis. Am J Physiol Heart Circ Physiol 295: H2512–2521.
40. Guo W, Wong S, Xie W, Lei T, Luo Z (2007) Palmitate modulates intracellular signaling, induces endoplasmic reticulum stress, and causes apoptosis in mouse 3T3-L1 and rat primary preadipocytes. Am J Physiol Endocrinol Metab 293: E576–586.
41. Harada K, Ogai A, Takahashi T, Kitakaze M, Matsubara H, et al. (2008) Crossveinless-2 controls bone morphogenetic protein signaling during early cardiomyocyte differentiation in P19 cells. J Biol Chem 283: 26705–26713.

Hypertension
JOURNAL OF THE AMERICAN HEART ASSOCIATION

Deficiency of Nectin-2 Leads to Cardiac Fibrosis and Dysfunction Under Chronic Pressure Overload

Seimi Satomi-Kobayashi, Tomomi Ueyama, Steffen Mueller, Ryuji Toh, Tomoya Masano, Tsuyoshi Sakoda, Yoshiyuki Rikitake, Jun Miyoshi, Hiroaki Matsubara, Hidemasa Oh, Seinosuke Kawashima, Ken-ichi Hirata and Yoshimi Takai

Hypertension. 2009;54:825-831; originally published online August 10, 2009;
doi: 10.1161/HYPERTENSIONAHA.109.130443
Hypertension is published by the American Heart Association, 7272 Greenville Avenue, Dallas, TX 75231

Print ISSN: 0194-911X. Online ISSN: 1524-4563

Deficiency of Nectin-2 Leads to Cardiac Fibrosis and Dysfunction Under Chronic Pressure Overload

Seimi Satomi-Kobayashi, Tomomi Ueyama, Steffen Mueller, Ryuji Toh, Tomoya Masano, Tsuyoshi Sakoda, Yoshiyuki Rikitake, Jun Miyoshi, Hiroaki Matsubara, Hidemasa Oh, Seinosuke Kawashima, Ken-ichi Hirata, Yoshimi Takai

Abstract—The intercalated disc, a cell-cell contact site between neighboring cardiac myocytes, plays an important role in maintaining the homeostasis of the heart by transmitting electric and mechanical signals. Changes in the architecture of the intercalated disc have been observed in dilated cardiomyopathy. Among cell-cell junctions in the intercalated disc, adherens junctions are involved in anchoring myofibrils and transmitting force. Nectins are Ca^{2+}-independent, immunoglobulin-like cell-cell adhesion molecules that exist in adherens junctions. However, the role of nectins in cardiac homeostasis and integrity of the intercalated disc are unknown. Among the isoforms of nectins, nectin-2 and -4 were expressed at the intercalated disc in the heart. Nectin-2–knockout mice showed normal cardiac structure and function under physiological conditions. Four weeks after banding of the ascending aorta, cardiac function was significantly impaired in nectin-2–knockout mice compared with wild-type mice, although both nectin-2–knockout and wild-type mice developed similar degrees of cardiac hypertrophy. Banded nectin-2–knockout mice displayed cardiac fibrosis more evidently than banded wild-type mice. The disruption of the intercalated discs and disorganized myofibrils were observed in banded nectin-2–knockout mice. Furthermore, the number of apoptotic cardiac myocytes was increased in banded nectin-2–knockout mice. In the hearts of banded nectin-2–knockout mice, Akt remained at lower phosphorylation levels until 2 weeks after banding, whereas c-Jun N-terminal kinase and p38 mitogen-activated protein kinase were highly phosphorylated compared with those of wild-type mice. These results indicate that nectin-2 is required to maintain structure and function of the intercalated disc and protects the heart from pressure-overload–induced cardiac dysfunction. (***Hypertension.* 2009;54:825-831.**)

Key Words: nectin-2 ■ cell adhesion molecule ■ intercalated disc ■ heart failure ■ pressure overload

In the mature heart, the intercalated discs are located at the bipolar ends of the rod-shaped cardiac myocytes and mediate mechanical and electric coupling between adjacent cardiac myocytes.[1] The intercalated disc mainly consists of 3 junctional complexes: adherens junctions (AJs), desmosomes, and gap junctions. The role of AJs in the intercalated disc is to anchor myofibrils and to transmit the force developed by the contracting myofibril to neighboring cardiac myocytes. Desmosomes provide structural support by anchoring the intermediate filament system, and gap junctions provide intercellular communication via ions and small molecules. Changes in the intercalated disc architecture have been reported in mouse models for dilated cardiomyopathy (DCM), such as muscle LIM protein knockout (KO) mice and tropomodulin-overexpressing mice.[2,3] On the other hand, the targeted ablation of N-cadherin, which is predominantly localized at AJs in the intercalated disc, in the murine adult was shown to result in the disassembly of the intercalated disc structure and to exhibit a DCM-like phenotype.[4] There are also several reports that the conditional KO mice of other AJ proteins in the heart, such as α-E-catenin,[5] mXin-α,[6] and vinculin,[7] showed cardiac dysfunction with the disruption of the intercalated disc. These findings suggest that AJ proteins are indispensable for the homeostasis of the intercalated disc and cardiac function.

Nectins are Ca^{2+}-independent, immunoglobulin-like cell-cell adhesion molecules found in AJs.[8,9] Nectins are a family composed of 4 members, nectin-1, -2, -3, and -4. All of the

Received February 15, 2009; first decision March 9, 2009; revision accepted July 20, 2009.

From the Division of Cardiovascular Medicine, Department of Internal Medicine (S.S-K., R.T., T.M., S.K., K-i.H.), and Division of Molecular and Cellular Biology, Department of Biochemistry and Molecular Biology (Y.R., Y.T.), Kobe University Graduate School of Medicine, Kobe, Japan; Department of Cardiovascular Medicine (T.U., H.M.), Kyoto Prefectural University of Medicine, Kyoto, Japan; Department of Experimental Therapeutics (T.U., H.M., H.O.), Translational Research Center, Kyoto University Hospital, Kyoto, Japan; Department of Molecular Genetics and Microbiology (S.M.), State University of New York at Stony Brook, Stony Brook, NY; Division of Coronary Heart Disease (T.S.), Department of Internal Medicine, Hyogo College of Medicine, Nishinomiya, Japan; Department of Molecular Biology (J.M.), Osaka Medical Center for Cancer and Cardiovascular Diseases, Osaka, Japan; Department of Molecular Biology and Biochemistry (Y.T.), Osaka University Graduate School of Medicine/Faculty of Medicine, Suita, Japan.

Correspondence to Tomomi Ueyama, Department of Cardiovascular Medicine, Kyoto Prefectural University of Medicine, 465 Kajii-cho Kawaramachi-Hirokoji, Kamigyo-ku, Kyoto 602-8566, Japan. E-mail toueyama-circ@umin.ac.jp

Hypertension **is available at http://hyper.ahajournals.org** **DOI: 10.1161/HYPERTENSIONAHA.109.130443**

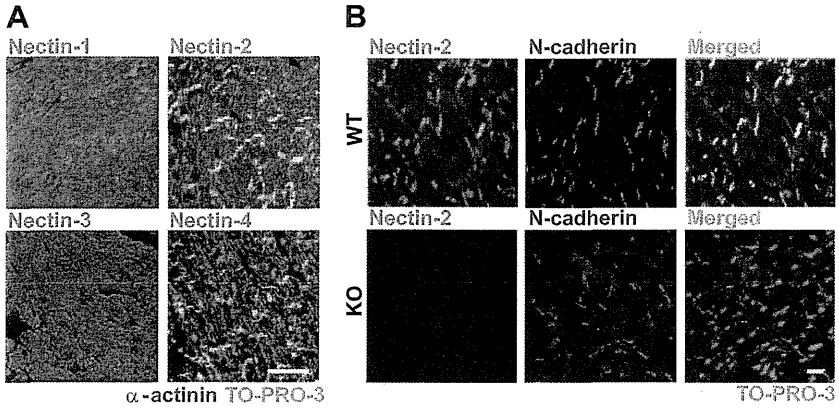

Figure 1. Localization of nectins and other proteins in the murine hearts. Frozen sections of the murine hearts at 4 weeks after banding were stained with the anti-α-actinin and N-cadherin antibodies (red); anti-nectin-1, -2, and -3 antibodies (green). Nuclei were stained with TO-PRO-3 (blue). A, Nectin-2 was specifically expressed in the intercalated disc. Bar, 50 μm. B, Nectin-2 was coexpressed with N-cadherin, which localized to the AJ, in the WT mouse hearts but not in the nectin-2–KO mouse hearts. Bar, 10 μm.

nectins form homo-*cis*-dimers and then homo- or hetero-*trans*-dimers through the extracellular region in a Ca^{2+}-independent manner, causing cell-cell adhesion. The cytoplasmic region is associated with the actin cytoskeleton through afadin, a nectin and actin filament (F-actin) binding protein. Nectins first form cell-cell adhesion and recruit cadherins to the nectin-based cell-cell adhesion sites, and this leads to the formation of AJs. Thus, nectins are important for the formation of AJs.

Among the isoforms of nectins, nectin-2 is known to exist in the heart.[10] However, the role of nectin-2 in the heart remains to be elucidated. The present study shows critical roles for nectin-2 in the heart under pressure overload.

Materials and Methods

Animal Experiments

Animal care and experiments were conducted according to guidelines for animal experimentation at Kobe University. Nectin-2–KO mice were generated as described previously, but the cardiac phenotype of the mice was not assessed in detail.[11] Ascending aortic constriction was performed in male wild-type (WT) or nectin-2–KO mice at the age of 11 weeks, as described previously,[12] except that the aorta was ligated with a 26-gauge needle. The mice were euthanized at the indicated time points.

The following materials and methods used for this study are described in detail in the online Data Supplement (please see http://hyper.ahajournals.org): echocardiography and electrocardiography, antibodies, histological analysis, Western blotting, real-time PCR, and statistics.

Results

Expression and Localization of Nectins and Other Proteins in the Intercalated Disc

To examine the expression and localization of nectins in the murine heart, immunostaining of nectin-1, -2, -3, and -4 was performed. As shown in Figure 1A, nectin-2 and -4 were selectively localized to the intercalated discs of the WT mouse hearts, whereas nectin-1 or -3 was not detected. Western blotting showed no compensatory increase of nectin-1, -3, or -4 expression in the nectin-2–KO mouse hearts (Figure S1).

In the intercalated disc structure, nectin-2 was colocated with N-cadherin in the WT mouse hearts, indicating that nectin-2 exists in AJs of the intercalated discs (Figure 1B). The *trans*-interactions of nectins were reported to initiate and enhance the formation of cadherin-based AJs in epithelial cells.[8] However, the deficiency of nectin-2 affected neither N-cadherin expression and distribution nor the structure of the intercalated disc depicted by N-cadherin fluorescence (Figure 1B). Other AJ proteins, such as α-catenin, β-catenin, and afadin, as well as connexin43 (Cx43), a gap junction protein, were also present and distributed normally in the intercalated discs in the nectin-2–KO mouse hearts (Figure S2). These findings suggest that nectin-2 might not be essential for the development of the intercalated discs or the expression of other AJ and GP proteins.

Cardiac Hypertrophy and Dysfunction Induced by Pressure Overload in Nectin-2–KO Mice

The functional phenotypes of the nectin-2–KO mouse heart were investigated under physiological conditions. The heart weights of nectin-2–KO mice were similar to those of the WT mice (Figure S3, see sham-operated groups), and normal systolic function assessed by echocardiography was observed in nectin-2–KO mice (Table and Figure 2A, see sham-operated groups), suggesting that nectin-2–KO mice exhibit normal cardiac function under physiological conditions. The function of nectin-2 was then explored in the heart under pathological conditions. A left ventricular (LV) pressure-overload model was used in nectin-2–KO and WT mice to assess cardiac dimensions and function. The heart weights of WT and nectin-2–KO mice were

Table. Echocardiographic Assessment

	WT		KO	
Data	Sham (n=8)	Banding (n=13)	Sham (n=8)	Banding (n=13)
BW, g	27.2±0.4	27.1±0.5	27.5±0.4	27.2±0.4
IVS, mm	0.92±0.02	1.12±0.04*	0.93±0.02	1.13±0.04*
LVPW, mm	0.97±0.05	1.14±0.04*	0.91±0.02	1.09±0.02*
LVEDD, mm	2.11±0.08	2.80±0.12*	2.10±0.10	3.05±0.10*
LVESD, mm	1.04±0.05	1.60±0.09*	1.07±0.07	2.03±0.10*†
FS, %	51±1	43±1*	49±2	33±2*†
AoPg, mm Hg	5.2±1.0	28.1±2.5*	5.5±0.8	25.0±3.3*

BW indicates body weight; IVS, interventricular septum thickness; LVPW, LV diastolic posterior wall thickness; LVEDD, LV end-diastolic dimension; LVESD, LV end-systolic dimension; FS, fractional shortening; AoPg; aortic pressure gradient. Values are expressed as mean±SE.

*$P<0.05$ vs sham.

†$P<0.05$ vs banded WT mice.

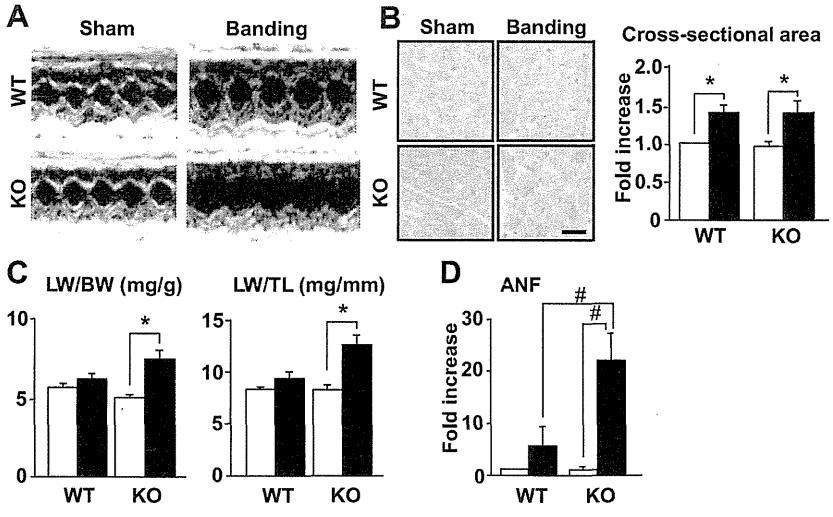

Figure 2. Alterations in cardiac dimensions and function under pressure overload in WT and nectin-2–KO mice. Cardiac dimensions and function were measured at 4 weeks after banding. White bars and black bars indicate sham-operated and aortic banding-operated mice, respectively. A, representative M-mode LV echocardiographic recording of WT mice (top) and nectin-2–KO mice (bottom) at 4 weeks after banding. B, left, Representative staining of cardiac sections with hematoxylin and eosin. Bar, 10 μm. Right, Cross-sectional areas of cardiac myocytes evaluated using ImageJ software (National Institutes of Health). The graphs represent fold increases of the myocyte area in the sham-operated WT mouse hearts. C, left, Lung weight (LW)/body weight (BW; mg/g). Right, LW/tibial length (TL; mg/mm). D, mRNA expression of atrial natriuretic factor (ANF) in the hearts at 4 weeks after banding. The graphs represent fold increases of mRNA expression levels in the sham-operated WT mouse hearts. Banding-operated nectin-2–KO mice showed a significant increase in ANF mRNA expression. *$P<0.05$, #$P<0.01$. Numbers for each group in panels B and C are shown in the Table. In A and D, n=6 in each group.

increased significantly, and the degrees of hypertrophy were similar between WT and nectin-2–KO mice after aortic banding (Figure S3). Histological analysis showed that the increase in the cross-sectional areas of cardiac myocytes in nectin-2–KO mice under chronic pressure overload was similar to that in WT mice (Figure 2B). Echocardiographic measurements revealed similar extents of increases in LV wall thickness in nectin-2–KO mice with aortic banding compared with corresponding WT mice (Table and Figure 2A). However, LV end-diastolic dimension tended to be larger, and LV end-systolic dimension was significantly greater in banded nectin-2–KO mice than in those in banded WT mice (LV end-systolic dimension: 2.03±0.10 versus 1.60±0.09 mm; banded nectin-2-KO mice versus banded WT mice: $P<0.05$). Systolic function was significantly depressed in banded nectin-2–KO mice compared with banded WT mice (percentage of fractional shortening: 33±2 versus 43±1; banded nectin-2-KO mice versus banded WT mice: $P<0.05$; Table and Figure 2A). Furthermore, a significant increase in lung weight was observed in banded nectin-2–KO mice, whereas the lung weight in WT mice was not changed after banding, indicating that pulmonary congestion was induced by pressure overload in nectin-2–KO mice but not in WT mice (Figure 2C). The mRNA expression of atrial natriuretic factor (ANF), a marker of cardiac stress that is elevated in the heart in pathological hypertrophy or heart failure,[12,13] was significantly increased in banded nectin-2–KO mice compared with banded WT mice (Figure 2D). Taken together, these results suggest that nectin-2 plays important roles in the transition from cardiac hypertrophy to progressive heart failure under chronic pressure overload, although nectin-2 is not indispensable for the development of cardiac hypertrophy.

Evident Myocardial Fibrosis Induced by Pressure Overload in Nectin-2–KO Mice

To examine whether pressure overload could induce distinct pathological differences between WT and nectin-2–KO mice, Masson trichrome staining was performed on heart sections to evaluate cardiac fibrosis. As shown in Figure 3A and 3B, the pressure-overload model used in this study displayed mild cardiac fibrosis in banded WT mice compared with sham-operated WT mice. In sham-operated nectin-2–KO mice, there was no overt cardiac fibrosis. However, pressure overload induced severe and diffuse cardiac fibrosis in banded nectin-2–KO mice compared with banded WT mice (fibrosis area: 21.7±2.5% versus 4.8±0.8%; banded nectin-2-KO mice versus banded WT mice: $P<0.01$).

The mRNA expression levels of type I collagen in nectin-2–KO mouse hearts were boosted to 4-fold of those in WT mouse hearts at 4 days after banding (Figure 3C). We also examined the mRNA expression levels of transforming growth factor-β, because this cytokine is known to be increased in the myocardium of hypertrophic cardiomyopathy, DCM, and myocardial infarction and is considered to induce cardiac fibrosis.[14,15] The levels of transforming growth factor-β1 mRNA in the banded nectin-2–KO mouse hearts were increased twice as much as those in the banded WT mouse hearts (Figure 3C).

Furthermore, to analyze the pathological features of diffuse and multifocal fibrosis in banded nectin-2–KO mice, cell death was assessed by TUNEL staining of cardiac sections. As shown in Figure 3D, the number of TUNEL-positive nuclei was more prominently increased in the banded nectin-2–KO mouse hearts than in the banded WT mouse hearts. These results suggest that nectin-2 has a protective role in cardiac myocytes against chronic pressure overload.

Disruption of Intercalated Discs in Nectin-2–KO Mice by Pressure Overload

Immunoblotting and immunofluorescence confocal microscopy were performed to examine the expression of component proteins and structural changes of the intercalated disc after banding. N-cadherin is well known to be present in the transmembrane part of AJs. On the cytoplasmic side of AJs, β-catenin binds to N-cadherin via the cytoplasmic domain,

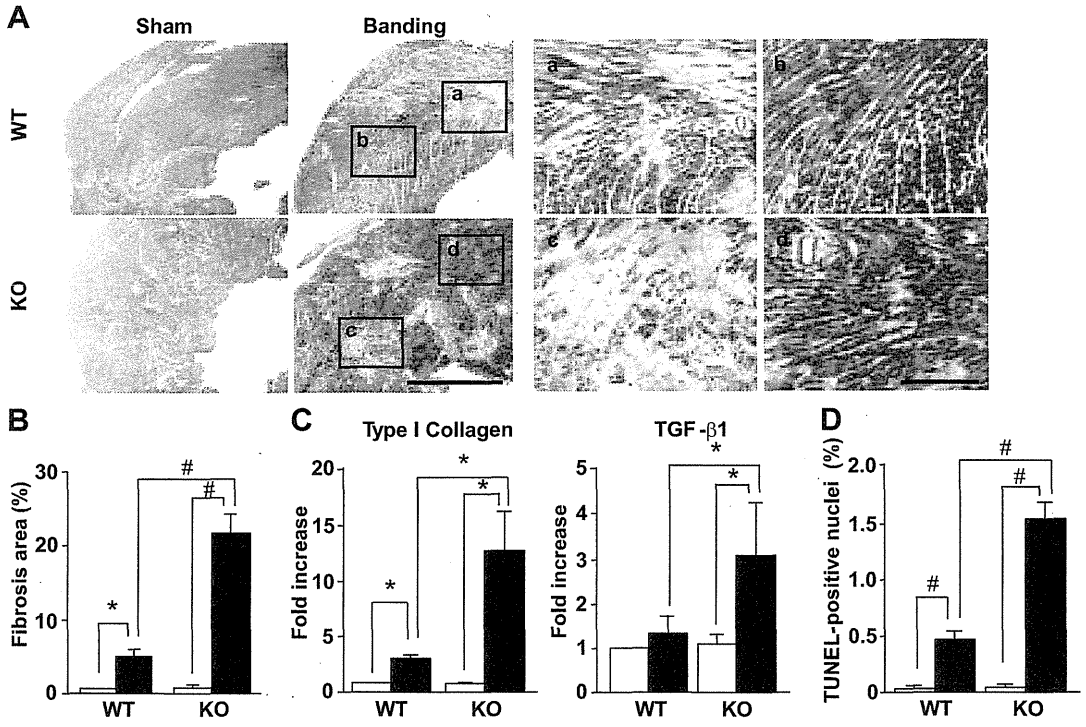

Figure 3. Myocardial fibrosis and apoptosis induced by pressure overload. White bars and black bars indicate sham-operated and aortic banding-operated mice, respectively. A, Heart sections from WT and nectin-2–KO mice were subjected to Masson trichrome staining at 4 weeks after banding. Left, Representative Masson trichrome staining. Bar, 1 mm. Right, Higher-magnification images. Bar, 300 μm. B, Quantitative analysis of the ratio of the myocardial fibrosis area to the total myocardial area (percentage). C, mRNA expression of type I collagen and transforming growth factor (TGF)-β1 in the hearts at 4 days after banding. The graphs represent fold increases in mRNA expression levels in the sham-operated WT mouse hearts. D, Ratio of the TUNEL-positive nuclei to the total nuclei in heart sections at 4 weeks after banding. *P<0.05, #P<0.01. n=6 in each group.

whereas it interacts with α-catenin at the other end. Then, α-catenin contacts the actin cytoskeleton. Deficiency of nectin-2 did not affect N-cadherin expression or distribution, even after banding (Figures 4A and S4). The notable change observed in the banded nectin-2–KO mouse hearts was the broader fluorescent line of the intercalated disc (Figure 4B). Such phenomena were reported in the hearts of DCM mice because of the higher degree of convolution of the plasma membrane in the intercalated disc.[3] For other AJ proteins, the expression and distribution of afadin, β1-integrin, and α-catenin in the heart did not differ between WT mice and nectin-2–KO mice after banding, whereas broad intercalated discs were observed similarly (Figure 4A and 4B). On the other hand, a gap junction protein (Cx43) expression in the banded hearts was reduced in both WT and nectin-2–KO mice (Figures S4 and 4A), whereas the distribution of Cx43 was not changed (Figure 4B). The expression of Cx43 in banded nectin-2–KO mouse hearts was significantly lower than that in banded WT mouse hearts (fold difference of sham-operated WT mice: 0.760±0.045 versus 0.438±0.040; banded WT mice versus banded nectin-2–KO mice after 4 weeks: P<0.05). To elucidate whether such a reduction in Cx43 causes electrocardiographic abnormality in nectin-2–KO mouse hearts, we performed electrocardiography (Figure S5). After banding, both WT and nectin-2–KO mice showed a prolonged QT interval to the same extent (Table S1), but no arrhythmia was observed in both WT and nectin-2–KO mice.

Transmission electron microscopy was performed to explore changes in the structure of the intercalated disc. As shown in Figure 4C, no significant change was observed in the structure of the intercalated disc in both sham-operated and banded WT mice. In sham-operated nectin-2–KO mice, the intercalated discs appeared intact. In banded nectin-2–KO mice, the intercalated discs were severely disrupted at only 2 weeks after the operation by the higher degree of membrane convolution that resembled the features of DCM, disarray of myofibrils, and disconnection from adjacent intercalated discs. These results suggest that nectin-2 is indispensable for maintaining the intercalated disc structure under chronic pressure overload.

Impaired Cellular Signalings in Nectin-2–KO Mice

Cell-cell junctions have important roles not only in cell adhesion but also in cell polarization, survival, movement, and proliferation via regulating signal transduction.[16] Because the activation of signaling molecules, such as extracellular signal–regulated kinase, c-Jun N-terminal kinase (JNK), p38 mitogen-activated protein kinase (MAPK), and Akt, has been reported to be associated with the development of the pressure-overload–induced hypertrophy and heart failure,[13,17] the activity of these molecules was examined after banding using Western blotting. The activation of extracellular signal–regulated kinase did not differ between WT and nectin-2–KO mice (Figure 5A). On the other hand, activation of JNK and

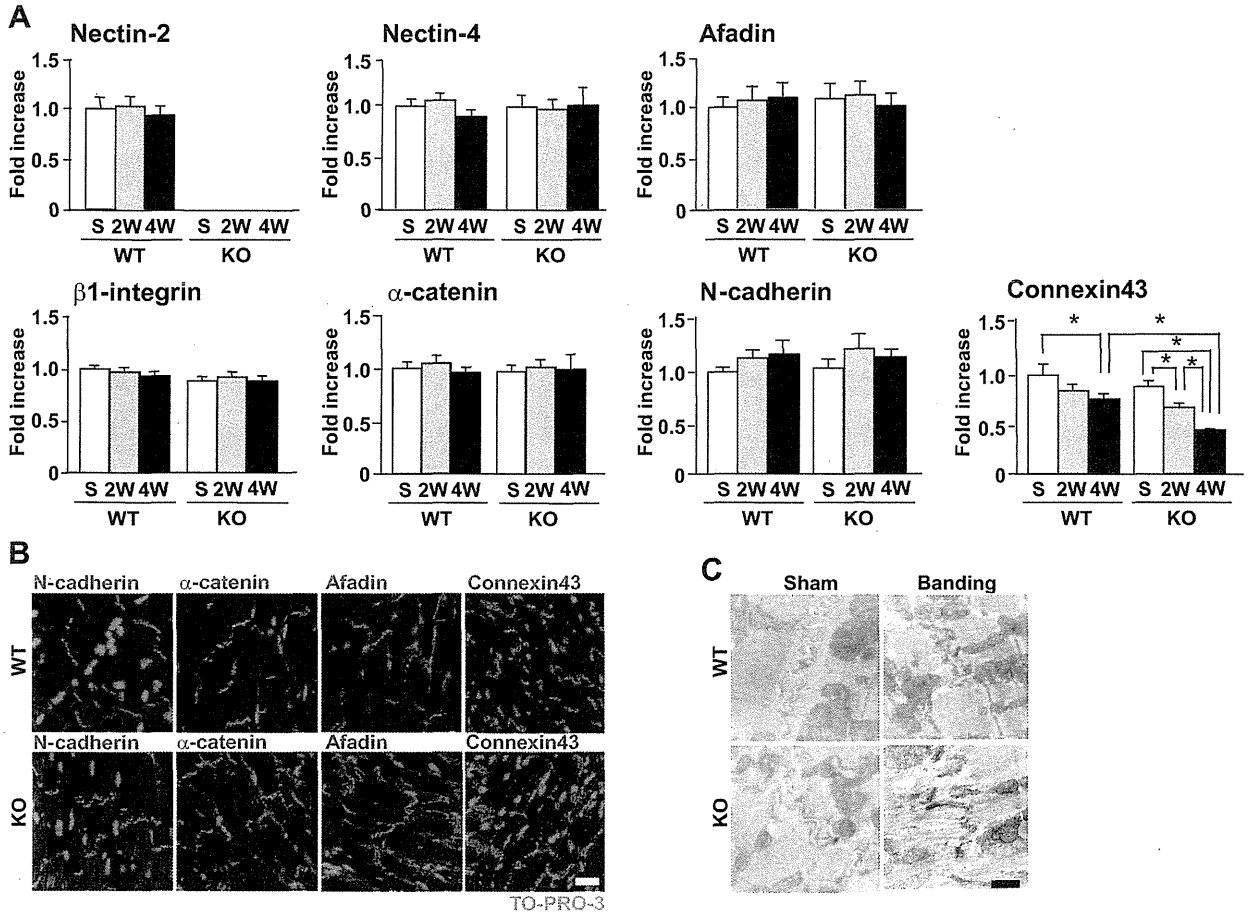

Figure 4. Pressure-overload–induced disruption of the intercalated discs in the nectin-2–KO mice. A, Graphs represent the fold increases in band intensities of Western blots of LV lysates. Each band was normalized by GAPDH as compared with the sham-operated WT mouse heart. White bars indicate sham-operated mice; gray bars indicate banding-operated mice after 2 weeks; black bars, after 4 weeks. n=6 to 8 in each group. B, Immunofluorescent staining for N-cadherin, α-catenin, afadin, and connexin43 in the hearts at 4 weeks after banding. Bar, 10 μm. C, Transmission electron microscope images of the myocardium at 2 weeks after banding. Bar, 1 μm.

p38 MAPK was more significant in nectin-2–KO mice than in WT mice after banding (Figure 5B and 5C). It is noteworthy that the activation of Akt was reduced more significantly in sham-operated nectin-2–KO mice than in sham-operated WT mice, and at 2 weeks after banding it decreased further in the nectin-2–KO mouse hearts (Figure 5D). However, Akt activation rose again and was increased further at 4 weeks after banding, although the significance of this finding was not further examined. These results indicate that nectin-2 is involved in intracellular signaling in the heart in response to chronic pressure overload.

Discussion

In the nectin-2–KO mouse hearts, the distribution and expression of the proteins localized in AJs, such as N-cadherin, α-catenin, β-catenin, afadin, and nectin-4, were unaffected. Because nectins have important roles in the recruitment of cadherins to the nectin-based cell-to-cell adhesion sites and the formation of AJs in epithelial cells,[8,9] nectin-4 in the nectin-2–KO mouse hearts may contribute to the recruitment and expression of AJ proteins. However, nectin-2–KO mice showed the disruption of the intercalated discs and the myofibril disarray after pressure overload, suggesting that nectin-4 alone does not compensate for the function of nectin-2 in the pressure-overloaded hearts. The digitation and convolution of the intercalated disc membrane in banded nectin-2–KO mice resembled the morphology observed in the DCM models.[2,3,18] Such changes in the intercalated-disc membrane between neighboring cardiac myocytes lead to a decrease in flexibility of the contractile tissue and an increased stiffness.[1] Therefore, these changes are in part attributable to cardiac dysfunction in banded nectin-2–KO mice. Expression of connexins in the failing myocardium is reduced in both animal models and human diseases.[19] We showed the reduction in Cx43 expression in the banded hearts of both WT and nectin-2–KO mice. The expression of Cx43 was significantly reduced in banded nectin-2–KO mouse hearts compared with banded WT mouse hearts. However, no arrhythmia was observed in nectin-2–KO mice even after banding. In selectively bred, cardiac-restricted Cx43-KO mice, reduction of Cx43 expression to 59% of matched controls does not induce susceptibility to arrhythmia, but

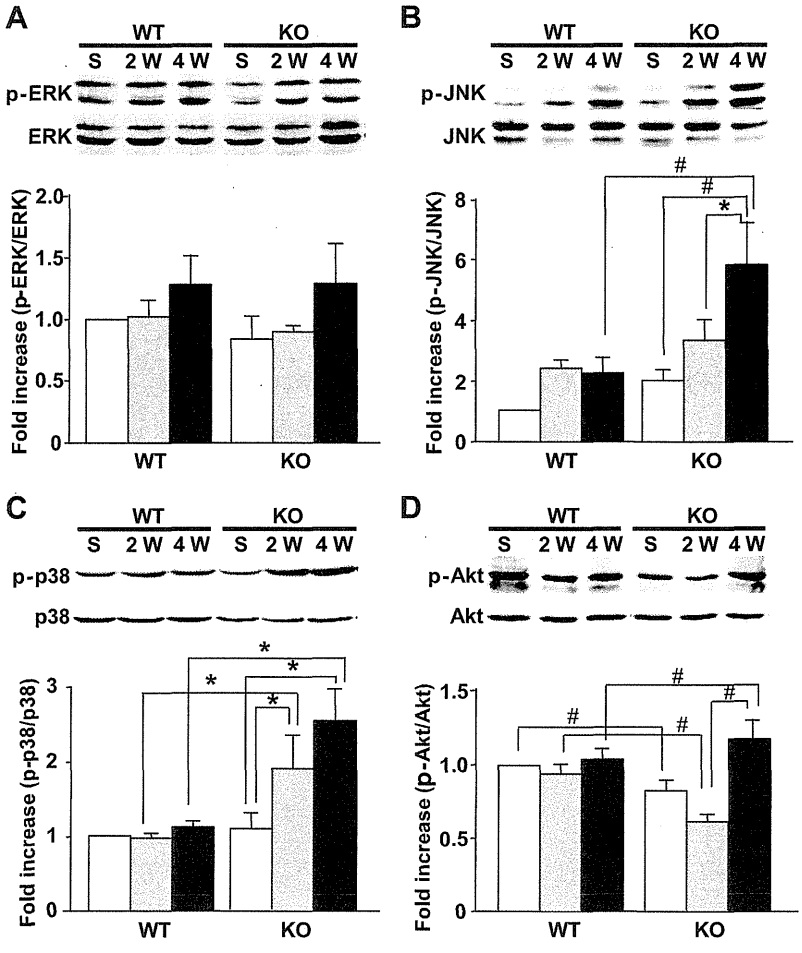

Figure 5. Impaired signal transduction in nectin-2–KO mice. Representative Western blots of LV lysates from different groups after banding. The graphs under each blot represent the fold increases in band intensities of phosphorylated extracellular signal–regulated kinase (ERK), JNK, p38 MAPK, and Akt normalized to the total amount of each protein as compared with the sham-operated WT mouse heart. White bars, Sham-operated mice; gray bars, banding-operated mice after 2 weeks; black bars, after 4 weeks. $^{*}P<0.05$, $\#P<0.01$. n=6 in each group.

when the Cx43 reduction reaches 18% of control levels, 80% of the mice are inducible into lethal ventricular arrhythmias,[20] implying that the reduction in Cx43 expression in banded nectin-2–KO mice might not be sufficient to induce arrhythmia.

Increased myocardial apoptosis, the resultant loss of cardiac myocytes, and consequential fibrosis are other mechanisms of cardiac dysfunction in banded nectin-2–KO mice. We considered that signaling impairment in nectin-2–KO mice heart provides some explanation for the distinguishing cell death and fibrosis. Extracellular signal–regulated kinase, JNK, p38 MAPK, and Akt have been reported to be activated under pressure overload.[12,21–23] The phosphorylation levels of JNK and p38 MAPK in the nectin-2–KO mouse hearts were notably increased after banding and were much higher compared with those in the WT mouse hearts at each corresponding time point. Recent in vivo experiments using genetically modified animals have provided insights into important aspects of MAPK activity in the heart. That is, JNK or p38 MAPK does not positively regulate cardiac hypertrophy in vivo but facilitates apoptosis and fibrosis.[24,25] Therefore, the JNK and p38 MAPK activation in nectin-2–KO mice may contribute to apoptosis of cardiac myocytes and the process of fibrotic changes in the heart under pressure overload. The nectin-3–afadin system regulates phosphatidylinositol 3-kinase-Akt signaling induced by the platelet-derived growth factor.[26] We showed that the phosphorylation level of Akt was significantly lower in the nectin-2–KO mouse hearts than in the WT mouse hearts even before the operation, which continued until 2 weeks after the operation (Figure 5D), suggesting that nectin-2 in the heart regulates Akt signaling. Akt is involved in the survival of various types of cells,[27–29] and Akt1-KO mice and transgenic mice expressing dominant-negative phosphatidylinositol 3-kinase with the reduced Akt activity under basal conditions display an accelerated heart failure phenotype to pressure overload.[30,31] Impaired activation of Akt in the nectin-2–KO mouse hearts may be involved in the increased susceptibility of cardiac myocytes to apoptosis after banding. We also showed that the phosphorylation level of Akt at 4 weeks after banding was even greater in the nectin-2–KO mouse hearts than in the WT mouse hearts. A possible explanation is provided with the evidence that Akt is usually activated in a failing myocardium, which is regarded as a compensatory reaction.[32] Because Akt is regulated by various upstream molecules because of its critical role in cell survival, signaling molecules regulating Akt activation, conceivably from the costameres, are likely to be upregulated at the stage of heart failure.

Perspectives

The present results indicate that nectin-2 plays a protective role in the heart against cardiac dysfunction induced by

pressure overload. The effect of nectin-2 is considered to be unique and independent from other AJ proteins. Additional analysis of the roles of nectin-2 and other proteins in the intercalated disc may contribute to deepen our understanding of the complicated mechanisms of heart failure.

Acknowledgments

We thank Toshiko Kojima for technical assistance.

Sources of Funding

This work was supported in part by grants from the Ministry of Education, Culture, Sports, Science, and Technology of Japan (to S.S-K., T.U., and R.T.); Grants-in-Aid for Scientific Research and for Cancer Research from the Ministry of Education, Culture, Sports, Science, and Technology of Japan (to Y.T.); the Takeda Science Foundation (to T.U.), the Mitsubishi Pharma Research Foundation (to T.U. and Y.R.), and the Mochida Memorial Foundation for Medical and Pharmaceutical Research (to Y.R.).

Disclosures

None.

References

1. Perriard JC, Hirschy A, Ehler E. Dilated cardiomyopathy: a disease of the intercalated disc? *Trends Cardiovasc Med.* 2003;13:30–38.
2. Sussman MA, Welch S, Gude N, Khoury PR, Daniels SR, Kirkpatrick D, Walsh RA, Price RL, Lim HW, Molkentin JD. Pathogenesis of dilated cardiomyopathy: molecular, structural, and population analyses in tropomodulin-overexpressing transgenic mice. *Am J Pathol.* 1999;155: 2101–2113.
3. Ehler E, Horowits R, Zuppinger C, Price RL, Perriard E, Leu M, Caroni P, Sussman M, Eppenberger HM, Perriard JC. Alterations at the intercalated disk associated with the absence of muscle LIM protein. *J Cell Biol.* 2001;153:763–772.
4. Kostetskii I, Li J, Xiong Y, Zhou R, Ferrari VA, Patel VV, Molkentin JD, Radice GL. Induced deletion of the N-cadherin gene in the heart leads to dissolution of the intercalated disc structure. *Circ Res.* 2005;96:346–354.
5. Sheikh F, Chen Y, Liang X, Hirschy A, Stenbit AE, Gu Y, Dalton ND, Yajima T, Lu Y, Knowlton KU, Peterson KL, Perriard JC, Chen J. α-E-catenin inactivation disrupts the cardiomyocyte adherens junction, resulting in cardiomyopathy and susceptibility to wall rupture. *Circulation.* 2006;114:1046–1055.
6. Gustafson-Wagner EA, Sinn HW, Chen YL, Wang DZ, Reiter RS, Lin JL, Yang B, Williamson RA, Chen J, Lin CI, Lin JJ. Loss of mXinα, an intercalated disk protein, results in cardiac hypertrophy and cardiomyopathy with conduction defects. *Am J Physiol Heart Circ Physiol.* 2007; 293:H2680–H2692.
7. Zemljic-Harpf AE, Miller JC, Henderson SA, Wright AT, Manso AM, Elsherif L, Dalton ND, Thor AK, Perkins GA, McCulloch AD, Ross RS. Cardiac-myocyte-specific excision of the vinculin gene disrupts cellular junctions, causing sudden death or dilated cardiomyopathy. *Mol Cell Biol.* 2007;27:7522–7537.
8. Takai Y, Nakanishi H. Nectin and afadin: novel organizers of intercellular junctions. *J Cell Sci.* 2003;116:17–27.
9. Takai Y, Irie K, Shimizu K, Sakisaka T, Ikeda W. Nectins and nectin-like molecules: roles in cell adhesion, migration, and polarization. *Cancer Sci.* 2003;94:655–667.
10. Takahashi K, Nakanishi H, Miyahara M, Mandai K, Satoh K, Satoh A, Nishioka H, Aoki J, Nomoto A, Mizoguchi A, Takai Y. Nectin/PRR: an immunoglobulin-like cell adhesion molecule recruited to cadherin-based adherens junctions through interaction with Afadin, a PDZ domain-containing protein. *J Cell Biol.* 1999;145:539–549.
11. Mueller S, Rosenquist TA, Takai Y, Bronson RA, Wimmer E. Loss of nectin-2 at Sertoli-spermatid junctions leads to male infertility and correlates with severe spermatozoan head and midpiece malformation, impaired binding to the zona pellucida, and oocyte penetration. *Biol Reprod.* 2003;69:1330–1340.
12. McMullen JR, Shioi T, Zhang L, Tarnavski O, Sherwood MC, Kang PM, Izumo S. Phosphoinositide 3-kinase(p110α) plays a critical role for the induction of physiological, but not pathological, cardiac hypertrophy. *Proc Natl Acad Sci U S A.* 2003;100:12355–12360.
13. Hoshijima M, Chien KR. Mixed signals in heart failure: cancer rules. *J Clin Invest.* 2002;109:849–855.
14. Khan R, Sheppard R. Fibrosis in heart disease: understanding the role of transforming growth factor-beta in cardiomyopathy, valvular disease and arrhythmia. *Immunology.* 2006;118:10–24.
15. Bujak M, Frangogiannis NG. The role of TGF-β signaling in myocardial infarction and cardiac remodeling. *Cardiovasc Res.* 2007;74:184–195.
16. Rikitake Y, Takai Y. Interactions of the cell adhesion molecule nectin with transmembrane and peripheral membrane proteins for pleiotropic functions. *Cell Mol Life Sci.* 2008;65:253–263.
17. Bueno OF, Molkentin JD. Involvement of extracellular signal-regulated kinases 1/2 in cardiac hypertrophy and cell death. *Circ Res.* 2002;91: 776–781.
18. Arber S, Hunter JJ, Ross J Jr, Hongo M, Sansig G, Borg J, Perriard JC, Chien KR, Caroni P. MLP-deficient mice exhibit a disruption of cardiac cytoarchitectural organization, dilated cardiomyopathy, and heart failure. *Cell.* 1997;88:393–403.
19. Severs NJ, Bruce AF, Dupont E, Rothery S. Remodelling of gap junctions and connexin expression in diseased myocardium. *Cardiovasc Res.* 2008; 80:9–19.
20. Danik SB, Liu F, Zhang J, Suk HJ, Morley GE, Fishman GI, Gutstein DE. Modulation of cardiac gap junction expression and arrhythmic susceptibility. *Circ Res.* 2004;95:1035–1041.
21. Fischer TA, Ludwig S, Flory E, Gambaryan S, Singh K, Finn P, Pfeffer MA, Kelly RA, Pfeffer JM. Activation of cardiac c-Jun NH(2)-terminal kinases and p38-mitogen-activated protein kinases with abrupt changes in hemodynamic load. *Hypertension.* 2001;37:1222–1228.
22. Yasukawa H, Hoshijima M, Gu Y, Nakamura T, Pradervand S, Hanada T, Hanakawa Y, Yoshimura A, Ross J Jr, Chien KR. Suppressor of cytokine signaling-3 is a biomechanical stress-inducible gene that suppresses gp130-mediated cardiac myocyte hypertrophy and survival pathways. *J Clin Invest.* 2001;108:1459–1467.
23. Sadoshima J, Montagne O, Wang Q, Yang G, Warden J, Liu J, Takagi G, Karoor V, Hong C, Johnson GL, Vatner DE, Vatner SF. The MEKK1-JNK pathway plays a protective role in pressure overload but does not mediate cardiac hypertrophy. *J Clin Invest.* 2002;110:271–279.
24. Liang Q, Molkentin JD. Redefining the roles of p38 and JNK signaling in cardiac hypertrophy: dichotomy between cultured myocytes and animal models. *J Mol Cell Cardiol.* 2003;35:1385–1394.
25. Baines CP, Molkentin JD. STRESS signaling pathways that modulate cardiac myocyte apoptosis. *J Mol Cell Cardiol.* 2005;38:47–62.
26. Kanzaki N, Ogita H, Komura H, Ozaki M, Sakamoto Y, Majima T, Ijuin T, Takenawa T, Takai Y. Involvement of the nectin-afadin complex in PDGF-induced cell survival. *J Cell Sci.* 2008;121:2008–2017.
27. Kauffmann-Zeh A, Rodriguez-Viciana P, Ulrich E, Gilbert C, Coffer P, Downward J, Evan G. Suppression of c-Myc-induced apoptosis by Ras signalling through PI(3)K and PKB. *Nature.* 1997;385:544–548.
28. Datta SR, Dudek H, Tao X, Masters S, Fu H, Gotoh Y, Greenberg ME. Akt phosphorylation of BAD couples survival signals to the cell-intrinsic death machinery. *Cell.* 1997;91:231–241.
29. Cardone MH, Roy N, Stennicke HR, Salvesen GS, Franke TF, Stanbridge E, Frisch S, Reed JC. Regulation of cell death protease caspase-9 by phosphorylation. *Science.* 1998;282:1318–1321.
30. DeBosch B, Treskov I, Lupu TS, Weinheimer C, Kovacs A, Courtois M, Muslin AJ. Akt1 is required for physiological cardiac growth. *Circulation.* 2006;113:2097–2104.
31. McMullen JR, Amirahmadi F, Woodcock EA, Schinke-Braun M, Bouwman RD, Hewitt KA, Mollica JP, Zhang L, Zhang Y, Shioi T, Buerger A, Izumo S, Jay PY, Jennings GL. Protective effects of exercise and phosphoinositide 3-kinase(p110α) signaling in dilated and hypertrophic cardiomyopathy. *Proc Natl Acad Sci U S A.* 2007;104:612–617.
32. Haq S, Choukroun G, Lim H, Tymitz KM, del Monte F, Gwathmey J, Grazette L, Michael A, Hajjar R, Force T, Molkentin JD. Differential activation of signal transduction pathways in human hearts with hypertrophy versus advanced heart failure. *Circulation.* 2001;103:670–677.

ONLINE SUPPLEMENT

Deficiency of Nectin-2 Leads to Cardiac Fibrosis and Dysfunction under Chronic Pressure Overload

Seimi Satomi-Kobayashi,[1] Tomomi Ueyama,[2,3] Steffen Mueller,[4] Ryuji Toh,[1] Tomoya Masano,[1] Tsuyoshi Sakoda,[5] Yoshiyuki Rikitake,[6] Jun Miyoshi,[7] Hiroaki Matsubara,[2,3] Hidemasa Oh,[3] Seinosuke Kawashima,[1] Ken-ichi Hirata,[1] and Yoshimi Takai[6,8]

[1] Division of Cardiovascular Medicine, Department of Internal Medicine, Kobe University Graduate School of Medicine, Kobe 650-0017, Japan
[2] Department of Cardiovascular Medicine, Kyoto Prefectural University of Medicine, Kyoto 602-8566, Japan
[3] Department of Experimental Therapeutics, Translational Research Center, Kyoto University Hospital, Kyoto 606-8507, Japan
[4] Department of Molecular Genetics and Microbiology, State University of New York at Stony Brook, Stony Brook, New York 11794, USA
[5] Department of Internal Medicine, Division of Coronary Heart Disease, Hyogo College of Medicine, Nishinomiya 663-8501, Japan
[6] Division of Molecular and Cellular Biology, Department of Biochemistry and Molecular Biology, Kobe University Graduate School of Medicine, Kobe 650-0017, Japan.
[7] Department of Molecular Biology, Osaka Medical Center for Cancer and Cardiovascular Diseases, Osaka 537-8511, Japan
[8] Department of Molecular Biology and Biochemistry, Osaka University Graduate School of Medicine/Faculty of Medicine, Suita 565-0871, Japan

Short title: The Protective Role of Nectin-2 in the Heart

Abstract, 243 words. Manuscript, 4784 words and 5 figures and 1 table.

Correspondence to Tomomi Ueyama, MD, PhD, Department of Cardiovascular Medicine, Kyoto Prefectural University of Medicine, 465 Kajii-cho Kawaramachi-Hirokoji, Kamigyo-ku, Kyoto 602-8566, Japan. E-mail: toueyama-circ@umin.ac.jp; TEL: +81-75-251-5511; FAX: +81-75-251-5514

Materials and Methods

Echocardiography and Electrocardiography

Four weeks after aortic banding, echocardiography and electrocardiography were performed as described previously.[1,2] Mice anesthetized with 2,2,2-tribromoethanol (0.20 mg/g) by intraperitoneal injection were analyzed by echocardiogram and multilead-surface electrocardiogram. We used Envision C (PHILIPS) and JB-101J (Nihon Kohden, Tokyo, Japan) for experiments. M-mode recordings of the left ventricle were obtained at the level of the papillary muscles from a parasternal window.

Antibodies

Rat monoclonal anti–nectin-1, -2, and -3 antibodies (Abs), rabbit polyclonal anti–nectin-1, -3α Abs, and rabbit anti-l-afadin Abs were produced as described previously.[3,4] Rabbit polyclonal anti-nectin-4 Ab was produced using C-terminus (1111-1530) of nectin-4. Abs for phospho-Akt (Ser473), Akt, phospho-p44/42 MAP kinase (ERK1/2), p44/42 MAP kinase (ERK1/2), phospho-SAPK/JNK, SAPK/JNK, phospho-p38 MAPK, p38 MAPK (Cell Signaling Technology), N-cadherin, α-catenin, β-catenin (Zymed), α-actinin, connexin43 (BD Biosciences), and β1-integrin (SIGMA) were purchased.

Histological Analysis

Histological analysis of the hearts was performed as described previously.[2] Immunofluorescence microscopy was performed using a LSM5 Pascal microscope (Carl Zeiss). Nuclei were visualized using TO-PRO-3 (Molecular Probes) as described previously.[5] The area of cardiac myocytes was calculated by measuring at least 500 cells per mouse using ImageJ® software. Masson's trichrome staining was used to quantify fibrosis in the left ventricle (LV). The area of fibrosis was quantified using ImageJ® software and the fibrosis ratio was calculated by dividing the area of fibrosis by the total myocardial area. TUNEL reaction was performed on heart sections with an Apoptosis Detection Kit (Takara Bio). At least 10^4 nuclei from one heart section were counted to assess the ratio of TUNEL-positive nuclei to myocardial nuclei. For transmission electron microscopy, LV walls were fixed in Karnovsky's fixative (pH 7.4) (2% paraformaldehyde, 2.5% glutaraldehyde, 0.2 M phosphate buffered saline) for 2 h, postfixed with 1.5% OsO_4, dehydrated in graded ethanol, and embedded in Quetol 812. Thin sections were examined using a HITACHI H-600A electron microscope.

Western Blotting

Heart lysates were obtained by homogenization in ice-cold buffer (10 mM Tris-HCl (pH 7.4), 1 mM EDTA, 1 mM EGTA (pH 8.0), 150 mM NaCl, 0.5% Triton X-100, 0.2 mM sodium orthovanadate, 0.2 mM phenylmethylsulfonyl fluoride). The lysates were subjected to sodium dodecyl sulfate-polyacrylamide gel electrophoresis (SDS-PAGE) and proteins were transferred onto polyvinylidene difluoride (PVDF) membranes (Immobilon-P; Millipore). The bands were quantified

by densitometry analysis using ImageJ® software (n=6~8). L fibroblasts stably expressing nectin-1, nectin-2, and nectin-3 were used as the positive controls of each nectin.[6] Human umbilical vein endothelial cells were used as a positive control of nectin-4.

Real-Time PCR

Total RNA was isolated from left ventricular wall samples and real-time PCR was performed using an Applied Biosystems 7500 Real-Time PCR System (Applied Biosystems) with Takara One Step SYBR® RT-PCR Kit (Takara Bio). The following primers were designed by Takara Bio for murine atrial natriuretic factor (ANF) (forward, 5'-GGACTAGGCTGCAACAGCTTC-3'; reverse, 5'-GTGACACACCACAAGGGCTTA-3'), murine type I collagen (forward, 5'-ATGCCGCGACCTCAAGATG-3; reverse, 5'-TGAGGCACAGACGGCTGAGTA-3'), murine TGF-β1 (forward, 5'-GTGTGGAGCAACATGTGGAACTCTA-3'; reverse, 5'-TTGGTTCAGCCACTGCCGTA-3'), and murine GAPDH (forward, 5'-TGTGTCCGTCGTGGATCTGA-3'; reverse, 5'-TTGCTGTTGAAGTCGCAGGAG-3'). GAPDH was used for normalization, and the comparative threshold method was used to assess the relative abundance of the targets.

Statistics

All experiments were performed at least three times. Results are expressed as mean ± SEM. Differences between groups were compared using one-way analysis of variance, followed by Fisher's protected least significant difference post hoc test or Scheffe's post hoc test. A value of $p<$ 0.05 was considered significant.

References

1. Shioi T, Kang PM, Douglas PS, Hampe J, Yballe CM, Lawitts J, Cantley LC, Izumo S. The conserved phosphoinositide 3-kinase pathway determines heart size in mice. *EMBO J.* 2000;19:2537-2548.
2. Ogata T, Ueyama T, Isodono K, Tagawa M, Takehara N, Kawashima T, Harada K, Takahashi T, Shioi T, Matsubara H, Oh H. MURC, a muscle-restricted coiled-coil protein that modulates the Rho/ROCK pathway, induces cardiac dysfunction and conduction disturbance. *Mol Cell Biol.* 2008;28:3424-3436.
3. Takahashi K, Nakanishi H, Miyahara M, Mandai K, Satoh K, Satoh A, Nishioka H, Aoki J, Nomoto A, Mizoguchi A, Takai Y. Nectin/PRR: an immunoglobulin-like cell adhesion molecule recruited to cadherin-based adherens junctions through interaction with Afadin, a PDZ domain-containing protein. *J Cell Biol.* 1999;145:539-549.
4. Satoh-Horikawa K, Nakanishi H, Takahashi K, Miyahara M, Nishimura M, Tachibana K, Mizoguchi A, Takai Y. Nectin-3, a new member of immunoglobulin-like cell adhesion molecules that shows homophilic and heterophilic cell-cell adhesion activities. *J Biol Chem.* 2000;275:10291-10299.
5. Ueyama T, Kasahara H, Ishiwata T, Nie Q, Izumo S. Myocardin expression is regulated by Nkx2.5, and its function is required for cardiomyogenesis. *Mol Cell Biol.* 2003;23:9222-9232.
6. Shingai T, Ikeda W, Kakunaga S, Morimoto K, Takekuni K, Itoh S, Satoh K, Takeuchi M, Imai T, Monden M, Takai Y. Implications of nectin-like molecule-2/IGSF4/RA175/SgIGSF/TSLC1/SynCAM1 in cell-cell adhesion and transmembrane protein localization in epithelial cells. *J Biol Chem.* 2003;278:35421-35427.